Letter

Hydrothermal Synthesis of Quartz Nanocrystals

Jane F. Bertone, Joel Cizeron, Rajeev K. Wahi, Joan K. Bosworth, and Vicki L. Colvin

Nano Letters, **2003**, 3 (5), 655-659 • DOI: 10.1021/nl025854r

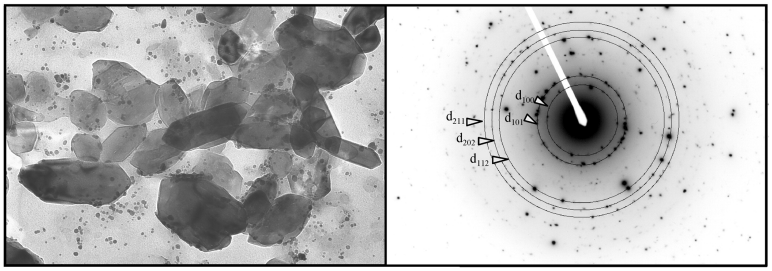

NANO LETTERS

2003
Vol. 3, No. 5
655−659

Hydrothermal Synthesis of Quartz Nanocrystals

Jane F. Bertone, Joel Cizeron, Rajeev K. Wahi, Joan K. Bosworth, and Vicki L. Colvin*

Department of Chemistry, Rice University, 6100 Main Street, Houston, Texas 77005

Received October 18, 2002; Revised Manuscript Received December 6, 2002

ABSTRACT

This paper describes for the first time a chemical method for the preparation for nanocrystalline quartz. Submicron quartz powders are initially produced in hydrothermal reactions where soluble silica precursors precipitate as pure crystalline silica. To yield nanocrystalline material these particles can be purified and size selected by dialysis, filtration, and centrifugation. Transmission electron microscopy and X-ray diffraction illustrate that the product is pure phase α-quartz, consisting of isolated (i.e., nonaggregated) nanocrystals. Depending on the size selection method, crystallites with average sizes of 10 to 100 nanometers can be recovered.

In nature, quartz is the primary form of silicon and oxygen, elements that together comprise over 70% of the earth's crust.[1] Its properties have been of great interest to geologists for decades, and its superior electrical and thermal insulating properties find applications in many industries.[2−5]

Given the widespread importance of quartz in nature and technology, it is remarkable that there are no reported chemical routes for the production of nanoscale quartz. Such a material would have a range of potential uses. The phase behavior of quartz nanocrystals could provide insight into the fundamental mechanisms responsible for solid-state amorphization and the $\alpha-\beta$ transition, and their solution phase properties would be a valuable model for rock erosion.[6−11] Nanoquartz might also exhibit nanoscale piezoelectric behavior, which could be applied in small-scale actuators and motors. These and other potential applications motivated us to develop a solution-phase route to form nanoquartz.

Quartz possesses features that make a purely chemical approach to its nanoscale formation challenging. First, the amorphous state of silica is nearly equal in energy to that of α-quartz.[12] Thus, the common nanochemical strategy of employing rapid decomposition of molecular precursors to form crystallites generally fails since the resulting product is amorphous. Second, the ideal prescription for nanocrystal formation, fast nucleation followed by slow growth, is difficult to implement in the case of quartz due to its extremely rapid growth rate in conditions required for its nucleation (80 nm/sec at 263 °C in 0.5 M NaOH).[13,14] This rapid growth rate also makes size control problematic.

For these reasons, our strategy relies on both chemical as well as physical methods to form nanocrystalline quartz.[15] We conduct our reactions under hydrothermal conditions where bulk quartz is known to precipitate from aqueous solutions saturated with silica. Hydrothermal reactions have been successful at producing other nanocrystalline oxides such as TiO_2 and $BaTiO_2$, and recent reports have highlighted hydrothermal synthesis of micron sized quartz powders.[8,16−21] Taking these as a starting point, we use high surface area silica precursors and perform the reaction under basic conditions in order to accelerate the quartz nucleation rate.[22−28] The resulting submicron powders can be subjected to simple purification processes which allow for nanocrystal samples of varying average sizes to be generated.

This reaction starts with the hydrothermal dissolution and reprecipitation of silica under conditions designed to encourage rapid nucleation of quartz. In a typical reaction, 3.5 g of a dry amorphous silica precursor is added to 100 mL 0.1 M NaOH in a Parr 4550 minireactor and ramped at 6 °C/min to 200−300 °C (see Supporting Information for detailed reaction procedures). Most of the reactions reported here use fumed silica as the starting material (99.8%, 390 m^2/g, Sigma), though amorphous colloidal silica gives equivalent results. Both of these silica sources have high surface areas which result in rapidly rising soluble silica levels in the reactor. This coupled with strong basic conditions favors quartz nucleation.

After 2 h, the starting product has dissolved and the reaction is quenched to 70 °C in 10−15 min by water circulation through the internal reactor cooling loop. A white powder (90% yield) can be recovered and purified by dialysis. It is crucial during dialysis to maintain a slightly basic pH (∼8). More basic solutions will favor the dissolution of solid phases of silica and may reduce the quartz yield.[29] Even slightly acidic solutions are known to promote the

* Corresponding author. E-mail: colvin@rice.edu

10.1021/nl025854r CCC: $25.00
Published on Web 03/27/2003

Table 1. Phases Observed under Different Conditions

precursor	*T* (°C)	time	product
F[a]	300	1 h 20 min	s[b]Q[c]
F	250	5 hr	WdQ
F	200	40 hr	C[e], wQ
S[f]	300	1 h 30 min	sQ
F-ethanol	200	12 hr	amorph

[a] fumed silica. [b] strong. [c] quartz. [d] weak. [e] cristobalite. [f] Stöber silica.

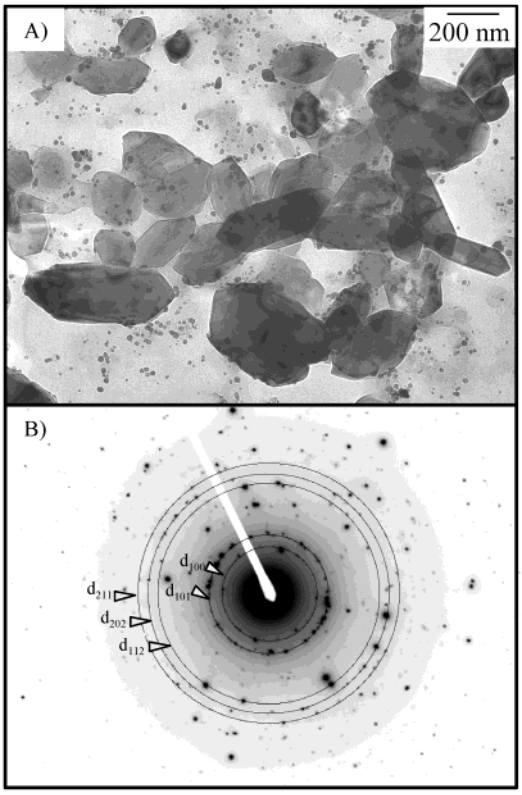

Figure 1. (A) TEM of the unfiltered product. (B) Selected area electron diffraction (SAED) pattern for the same type of sample. The rings indicated match to known quartz reflections. The reaction conditions are 3.5 g fumed silica for 2 h at 300 °C in 100 mL 0.1M NaOH.

coagulation of unreacted and amorphous particles which clog filters and aggregate the product.[30] Quartz precipitation occurs after time periods of 5 h or less when the reaction temperature is above 250 °C and the concentration of NaOH is 0.1 M. Table 1 shows that the solid product is pure phase quartz only over a narrow range of reaction conditions. As observed in the formation of large single crystals of quartz, lower temperatures and more neutral pH conditions result in unreacted amorphous product, the formation of cristobalite, or complex silicate phases.[31−33]

The quartz powders produced by this reaction contain submicron crystallites with a wide distribution of particle sizes (Figure 1). The product, after 2 h at 300 °C, is composed of many large faceted particles, some aggregates, and many smaller, nanometer scale solid particles that are relatively isolated (Figure 1A). Selected area electron diffraction (SAED) (Figure 1B) shows spots from single-crystal diffraction as well as faint rings from powder diffraction that

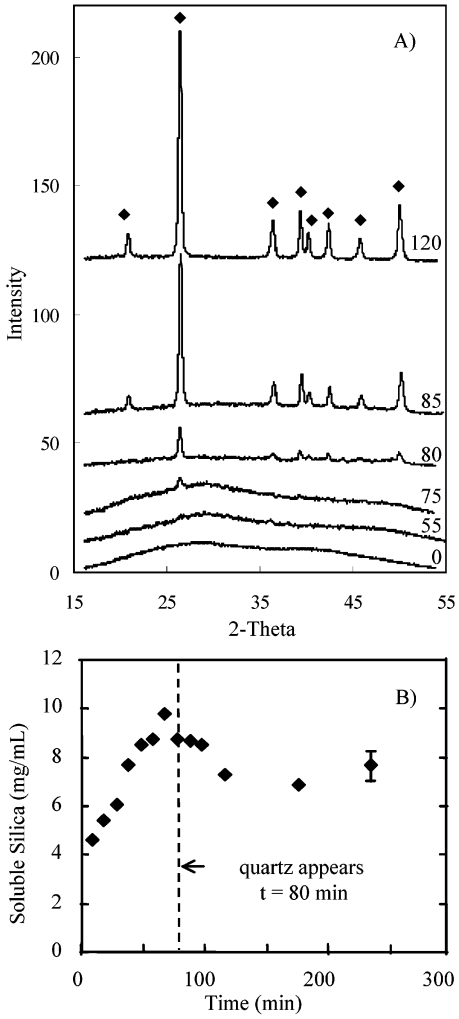

Figure 2. Reaction evolution. (A) SiO_2 phase evolution by X-ray diffraction (XRD) of samples quenched at different reaction times. The time of sampling is listed in minutes at the right of each pattern. Reflections marked by diamonds can all be indexed to α-quartz. No α-quartz reflections are absent. All reaction conditions were identical to those in Figure 1. (B) Concentration of dissolved silica derived from the absorbance of monomeric $Si(OH)_4$ complexed with molybdic acid (see Experimental Section in Supporting Information for more details). The error is 10% of $[Si(OH)_4]$ as indicated by the bar on the last data point.

can be indexed, in agreement with X-ray diffraction (XRD) (Figure 2A), to the expected reflections for quartz. Quartz powders are atomically pure as determined by energy-dispersive X-ray analysis (0.1 at. % Ti, 0.08 at. % Fe, 0.36 at. % Ni, and 0.13 at. % Cu). It is useful to acknowledge that though the goal of this investigation is production of nanoscale samples, this synthesis is one of few to report on quartz powders in the submicron length scale.[19−21]

As apparent in Figure 1A, nanocrystalline material comprises only a small fraction of the final quartz product; to assess whether nanocrystals were a major product at any time during the reaction we evaluated the time dependent growth of these particles (Figure 2).[15] Initially, a broad reflection characteristic of amorphous silica is observed (Figure 2A, bottom). During these early reaction times the soluble silica concentration steadily rises as the solid amorphous precursor dissolves (Figure 2B). After 70−90 min, when soluble silica

levels exceed 10 mg/mL, a narrow quartz reflection (superimposed on broader amorphous silica features) becomes visible at 26.65°. The width of this peak can be measured and from it a Scherrer fit is used to determine an average grain size of 31 nm.[34]

An additional 10 min of reaction produces powders that generate strong quartz patterns with over eight matching reflections (Figure 2A, 2nd from top). At this point the diffraction peaks are narrowed to the instrumental resolution limit and grain size analysis from such data is not feasible. These results illustrate that reaction quenching to limit crystallite size (such as extensive dilution after a brief period of nucleation) is not a productive strategy for nanocrystalline quartz. Quenched products contain significant fractions of amorphous silica as evidenced by the broad peaks in the X-ray diffraction data (Figure 2A). Also, with quartz growth rates of ~10 nm/second at the onset of nucleation, the separation of nucleation and growth does not occur in this reaction and thus crystals of very small size are only a small fraction of the product.

We run this reaction to near completion and use filtration and centrifugation to recover quartz nanocrystalline fractions. After dialysis, up to six different samples are combined and concentrated 8× by rotary evaporation. The samples are initially filtered over coarse filter paper (Whatman 541, Fisher Scientific) and then over a glass fiber prefilter (Millipore AP15, Fisher Scientific). The retentate from the glass filter yields fraction 1; the filtrate is then further size-selected by filtration over a 1.2 μm pore size nylon filter (Osmonics, Fisher Scientific) to give fraction 2. To yield smaller nanocrystals, these solutions are centrifuged for 2 min at 3313 G. The supernatant after this process provides a suspension of nanoquartz crystallites referred to as fraction 3. Fraction 4, the smallest fraction, is the supernatant after filtration over a 0.2 μm nylon filter (Osmonics) and centrifugation for 8 min at 3313 G. When such crystallites are in solution they are stable to sedimentation, colorless, and clear. In addition, when dried on a flat surface, the particles form a colorless clear thin film.

We found the combination of centrifugation and filtration to be necessary for reliable and efficient separations. Filtration alone is insufficient to produce reasonable size distributions because filter membranes do not provide strict cutoffs in size. Also, filters with very small pore sizes (0.025 μm, Millipore) tend to become clogged during filtration, which prohibits cake redispersal. Centrifugation alone is ineffective due to the breadth of the initial size distribution. By combining both techniques we were able to achieve the most efficient separation of smallest nanoquartz with no contamination from larger particles.

Transmission electron microscopy (TEM) illustrates that these size selection methods provide at least three different fractions of submicron to nanoscale α-quartz. Figure 3 shows the TEM data from both the supernatant (panel B) and pellet (panel A) of a sample that has been dialyzed, prefiltered, concentrated, and filtered over a 0.2-μm nylon membrane. This additional purification is able to remove large particles (>50 nm) as well as aggregates. Analysis of over 150

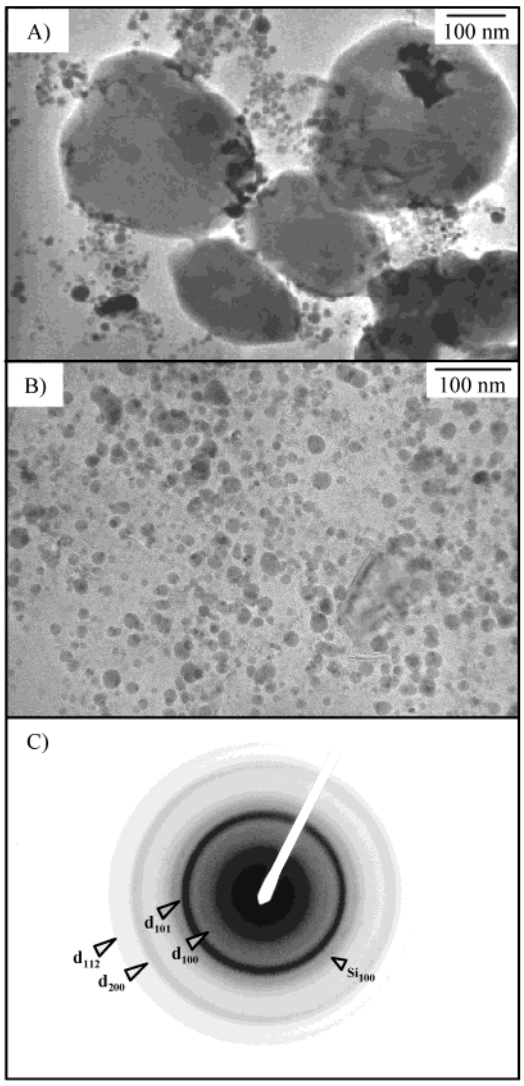

Figure 3. Size selection of quartz crystallites. (A) Transmission electron micrograph (TEM) of the redispersed pellet from a sample after it was dialyzed, prefiltered, concentrated, filtered over a 0.2 μm nylon membrane and centrifuged for 8 min at 3313 G (B) Fraction 4—the supernatant from the sample in panel A. (C) Selected area electron diffraction (SAED) Fraction 4. All reaction conditions were identical to those in Figure 1.

particles from TEM images allows us to determine the particle size distribution of the materials resulting from our separation procedures (Figure 4). The average size of each fraction decreases considerably from 440 nm in the largest samples to 18 nm in the smallest. Size distributions improve as particle sizes decrease, reaching 28% in the smallest fraction.

To verify that the small particles imaged in TEM were indeed α-quartz, we performed small area electron diffraction. The SAED results of these materials show rings, rather than spots, as expected for nanocrystalline samples; additionally, four quartz reflections were matched in the data (Figure 3C). High-resolution TEM images of nanocrystals can be found in the Supporting Information; they were less informative than the SAED in confirming the presence of quartz. Quartz has poor contrast in TEM due to its low electron density. Additionally, it is very sensitive to beam damage

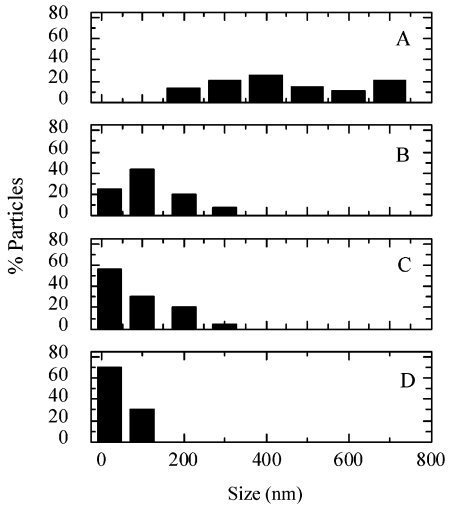

Figure 4. Sizing by TEM. Measurements were taken on the longest axis of at least 150 isolated particles. (A) Fraction 1 (retained from glass fiber prefilter) has an average size of 440 ± 228 nm. (B) Fraction 2 (filtered through 1.2 μm nylon paper, pellet after 20 min at 3313 G) has an average size of 84 nm and a size distribution from 1 to 175 nm. (C) Fraction 3 (filtered through 1.2 μm nylon paper, supernatant after 2 min at 3313 G) has an average size of 37 nm and a distribution from 1 to 83 nm. (D) Fraction 4 (the same sample as Figure 3B; filtered through 0.2 mm nylon paper, supernatant after 8 min at 3313 G) has an average size of 18 nm ± 5 nm. Reaction conditions were identical to Figure 1. All samples were dialyzed, concentrated and coarse paper filtered. Fractions 2−4 were also filtered over a glass fiber prefilter prior to further filtration as above.

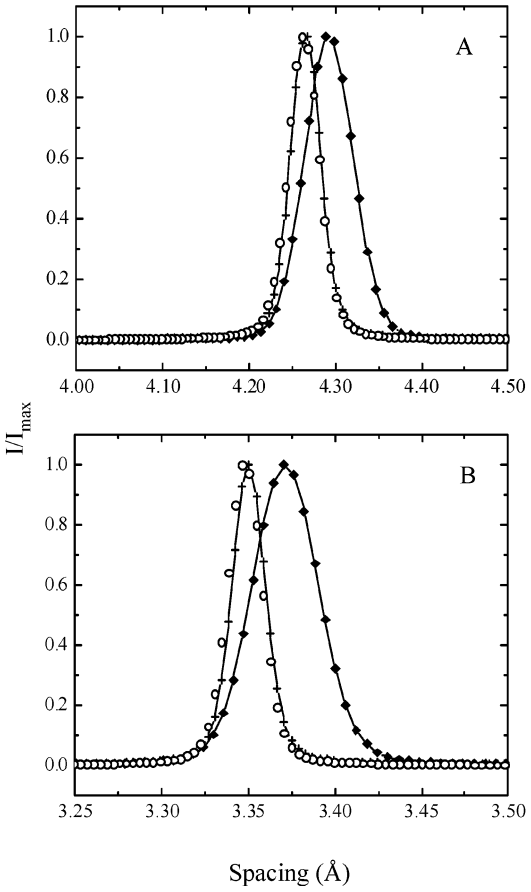

Figure 5. Sizing by XRD. (A) d_{101} peaks of the first three fractions shown in Figure 4. (B) d_{100} peaks of the same fractions. ○, fraction 1; +, fraction 2; ◆, fraction 3. Both d_{101} and d_{100} for fractions 1 and 2 are limited in peak width by the instrumental resolution. Scherrer analysis of fraction 3, d_{100} peak width gives a grain size of 28 nm while the d_{101} peak gives a grain size of 25 nm.[34]

in electron microscopes, forming silicon quite readily.[35−37] We found that the *d* spacing of the planes in high resolution images matched equally well to silicon as they did to quartz. We also found a weak reflection in the SAED that indexed to the Si 100 planes, but no evidence of silicon in X-ray diffraction data.

X-ray diffraction collected using a synchrotron X-ray source confirms the presence of nanocrystalline quartz. Samples were dried for synchrotron powder XRD, and the resulting reflections exhibit line broadening. The line widths for the (100) and (101) reflections of quartz are broadened considerably (Figure 5) in the smaller samples, to 0.18 and 0.20 degrees, respectively, as compared to the larger fractions in which peaks are narrowed to the instrumental resolution limit of 0.08 degrees measured using LaB_6 (NIST standard). Scherrer analysis of the d_{100} peaks finds a grain size of 28 nm for fraction 3. The reasonably good agreement between this grain size and the statistical particle size (37 nm) determined by TEM shown in Figure 4 is evidence that these small particles are indeed nanocrystalline quartz. Additionally, the agreement between the TEM and XRD grain size determinations suggests that particle defects and grain boundaries are not extensive in these materials. An analysis of this X-ray diffraction data, and its changes under pressure, are the subject of another publication.[38]

In this approach to forming nanoscale quartz, we sacrifice sample yield for phase purity and small size. While the yield of submicron quartz is ~90%, we typically recover less than 50 mg of solid material in our nanoscale fractions after combining product from several reactions. One reason this value is so low is the inefficiency of filtration; we lose many small particles during this step and a size selective precipitation scheme could provide one solution.[39] Colloidal silica has been shown to exhibit solute-dependent coagulation, which could be exploited in such a strategy.[29] Alternatively, quartz growth may be limited during the reaction through the addition of excess base. Existing data on the formation of zeolite colloids that form in hydrothermal reactors through precipitation of silicates suggest that excess OH^- enhances redissolution and retards the grain growth of aluminosilicates such as ZSM-5.[40] We find that increasing NaOH content substantially in this reaction yields complex silicate phases instead of quartz. Other bases, which do not contribute Na^+ to the reaction, may prove to be more useful.

Given the general success of hydrothermal methods in forming other nanoscale ceramics without size selection, it is useful to consider why quartz generates larger crystallites relative to other oxides such as titania. Reported surface energies for quartz range from 50 to 300 mJ/m^2 as compared to rutile and anatase TiO_2, which are 1.91 mJ/m^2 for rutile and 1.32 mJ/m^2 for anatase.[8,41,42] These high surface energies slow the homogeneous nucleation of quartz relative to titania.[43] Thus, the precipitation of quartz occurs after a long

delay during which the solution becomes supersaturated with silica (10 mg/mL as compared to the equilibrium solubility of 1 mg/mL at 300 °C), which enhances particle growth substantially.[29] Even if the solution were not saturated, crystal growth would occur quite rapidly. One report cites the growth rate for a large single crystal of quartz (in approximately 1.3 mg/mL aqueous silica, 263 °C) as 0.74 mm/day or 500 nm/min.[14] This value is comparable to the initial growth seen in the method we report where individual particles sizes reach 500 nm in roughly five minutes. In contrast, growth rates for hydrothermally synthesized TiO_2 nanoparticles are only a few Å/hr.[44] While the growth rates for single crystals can be quite different from the rates for powders, this comparison indicates why one would expect the hydrothermal precipitation of quartz to be very different from other ceramic materials.

We present the first report on the synthesis of nanoscale α-quartz. Isolated crystallites with characteristic nanoscale properties have been prepared by hydrothermal treatments of amorphous silica precursors. Quartz nanoparticles are isolated from polydisperse submicron quartz powders by pH controlled dialysis, filtration, and centrifugation. The average particle size and size distribution are significantly improved by this treatment. The smallest fraction isolated exhibits an average grain size of 18 nm with a size distribution of 5 nm. It is apparent from line broadening in X-ray diffraction that the average domain size of the nanocomponent is well below 100 nm. Scherrer analysis proves that quartz with average grain sizes below 37 nm can be formed. Furthermore, transmission electron microscopy and selected area electron diffraction show evidence of isolated quartz nanocrystals with an average size of 18 nm and a relatively narrow size distribution of 28%.

Acknowledgment. We thank Dr. Simon Clark and Mr. Stephen Prilliman, of Lawrence Berkeley Laboratories and UC Berkeley, respectively, for their assistance with synchrotron X-ray diffraction data. We acknowledge the National Center for Electron Microscopy at Lawrence Berkeley Laboratories for facilities useful for high resolution imaging of quartz nanocrystals. This work was supported by a Research Corporation Research Innovation Award, grant CHE-0103174 from the National Science Foundation, and the Robert A. Welch Foundation grant C-1342.

Supporting Information Available: Experimental details including dialysis purification, filtration, soluble silica concentration measurements, X-ray powder pattern collection and analysis, microscopy and energy-dispersive X-ray analysis; high-resolution transmission electron micrographs of fraction 4. This material is available free of charge via the Internet at http://pubs.acs.org.

References

(1) Mason, B.; Berry, L. G. *Elements of Mineralogy*; W. H. Freeman: San Francisco, 1968.
(2) Binggeli, N.; Chelikowsky, J. R. *Nature* **1991**, *353*, 344.
(3) Gillet, P. *Phys. Chem. Minerals* **1996**, *23*, 263.
(4) Hervey, P. R.; Foise, J. W. *Miner. Metallur. Proc.* **2001**, *18*, 1.
(5) Kingma, K. J.; Meade, C.; Hemley, R. J.; Mao, H. K.; Veblen, D. R. *Science* **1993**, *259*, 666.
(6) McHale, J. M.; Auroux, A.; Perrotta, A. J.; Navrotsky, A. *Science* **1997**, *277*, 788.
(7) Chun, C. C.; Herhold, A. B.; Johnson, C. S.; Alivisatos, A. P. *Science* **1997**, *276*, 398.
(8) Zhang, H.; Banfield, J. F. *J. Mater. Chem.* **1998**, *8*, 2073.
(9) Rios, S.; Salje, E. K. H.; Redfern, S. A. T. *Euro. Phys. J. B* **2001**, *20*, 75.
(10) Ullman, W. J.; Kirchman, D. L.; Welch, S. A.; Vandevivere, P. *Chem. Geo.* **1996**, *132*, 11.
(11) Bennet, P. C.; Melcer, M. E.; Siegel, D. I.; Hassett, J. P. *Geochem. Cosmochem. Acta* **1988**, *52*, 1521.
(12) Varshneya, A. K. *Fundamentals of Inorganic Glasses*; Academic Press: San Diego, 1994.
(13) LaMer, V. K.; Dinegar, R. H. *J. Am. Chem. Soc.* **1950**, *72*, 4847.
(14) Christov, M.; Kirov, G. C. *J. Cryst. Growth* **1993**, *131*, 560.
(15) We use the definition of "nano" to mean $d < 100$ nm (as given in: Roco, M. C.; Williams, S.; Alivisatos, A. P. *Nanotechnology Research Directions: IWGN Workshop Report*; WTEC, Loyola College Maryland, 1999) Particles from 100 to 1000 nm we refer to as submicron.
(16) Basca, R. R.; Gratzel, M. *J. Am. Ceram. Soc.* **1996**, *79*, 2185.
(17) Cheng, H.; Ma, J.; Zhao, Z.; Qi, L. *Chem. Mater.* **1995**, *7*, 663.
(18) Xia, C. T.; Shi, E. W.; Zhong, W. Z.; Guo, J. K. *J. Cryst. Growth* **1996**, *166*, 961.
(19) Balitsky, V. S.; Bublikova, T. M.; Marina, E. A.; Balitskaya, L. V.; Chichagova, Z. S.; Iwasaki, H.; Iwasaki, F. *High Press. Res.* **2001**, *20*, 273.
(20) Korytkova, E. N.; Chepik, L. F.; Mashchenko, T. S.; Drozdova, I. A.; Gusarov, V. V. *Inorg. Mater.* **2002**, *38*, 227.
(21) Lee, K. J.; Seo, K. W.; Y, H. S.; Mok, Y. I. *Korean J. Chem. Eng.* **1996**, *13*, 489.
(22) Campbell, A. S.; Fyfe, W. S. *Am. Mineral.* **1960**, *45*, 464.
(23) Fyfe, W. S.; McKay, D. S. *Am. Mineral.* **1962**, *47*, 83.
(24) Corwin, J. F.; Herzog, A. H.; Owen, G. E.; Yalman, R. G.; Swinnnerton, A. C. *J. Am. Chem. Soc.* **1953**, *73*, 3933.
(25) Eapen, M. J.; Reddy, K. S. N.; Shiralkar, V. P. *Zeolites* **1994**, *14*, 295.
(26) Helmkamp, M. M.; Davis, M. E. *Annu. Rev. Mater. Sci.* **1995**, *25*, 161.
(27) Lechert, H.; Kacirek, H. *Zeolites* **1993**, *13*, 192.
(28) Lavallo, M. C.; Tsapatsis, M. *Advanced Catalysts and Nanostructured Materials*; Academic Press: San Diego, 1996.
(29) Iler, R. K. *The Chemistry of Silica*; Wiley: New York, 1979.
(30) Bergna, H., Ed. *The Colloid Chemistry of Silica*; American Chemical Society: Washington, DC, 1994; Vol. 234.
(31) Carr, R. M.; Fyfe, W. S. *Am. Mineral.* **1958**, *43*, 909.
(32) Davis, M. E. *Strategies for Zeolite Synthesis by Design*; Elsevier Science B. V., 1995.
(33) Laudise, R. A. *J. Am. Chem. Soc.* **1958**, *81*, 562.
(34) Cullity, B. D. *Elements of X-ray Diffraction*, 2nd ed.; Addison-Wesley: Reading, 1978.
(35) Ashwell, W. B.; Todd, C. J.; Heckingbottom, R. *J. Phys. E* **1973**, *6*, 435.
(36) Pignatel, G. U.; Queirolo, G. *Rad. Eff.* **1983**, *79*, 291.
(37) Pitts, J. R.; Czanderna, A. W. *Nucl. Inst. Meth. Phys. Res.* **1986**, *B13*, 245.
(38) Bertone, J. F. et al., in preparation for submistion to Phys. Rev. B.
(39) Murray, C. B.; Norris, D. J.; Bawendi, M. G. *J. Am. Chem. Soc.* **1993**, *115*, 8706.
(40) Yamamura, M.; Chaki, K.; Wakatsuki, T.; Okado, H. *Zeolites* **1994**, *17*, 643.
(41) Janczuk, B.; Zdziennicka, B. *J. Mater. Sci.* **1994**, *29*, 3559.
(42) Parks, G. A. *J. Geophys. Res.* **1984**, *89*, 3997.
(43) Kashchiev, D. *Nucleation: Basic Theory with Applications*; Butterworth Heinemann: Oxford, 2000.
(44) Yanquing, Z.; Erwei, S.; Zhizhan, C.; Wenjun, L.; Xinfang, H. *J. Mater. Sci.* **2000**, *11*, 1547.

NL025854R